Electronic Supplementary Material (ESI) for Journal of Materials Chemistry A.

Supporting Information for

Crystallographic-plane tuned Prussian-blue wrapped with RGO: A high-capacity, long-life cathode for sodium-ion batteries

Hui Wang[a], Li Wang[b], Shuangming Chen[c], Guopeng Li[a], Junjie Quan[a], Enze Xu[a], Li Song*[c], Yang Jiang *[a]

[a.] *Dr. Hui Wang, Dr. Guopeng Li, Dr. Junjie Quan, Dr.Enze Xu, Prof. Yang Jiang*

*School of Materials Science and Engineering, Hefei University of Technology,Hefei, Anhui 230009, P. R. China.*E-mail: apjiang@hfut.edu.cn*

[b.] *Dr. Li Wang*

School of Chemistry and Chemical Engineering, Hefei University of Technology，Hefei, Anhui 230009, P. R. China

[c.] *Dr. Shuangming Cheng, Prof. Li Song*

National Synchrotron Radiation Laboratory, CAS Hefei Science Center, University of Science and Technology of China, Hefei 230029, China.

E-mail:song2012@ustc.edu.cn

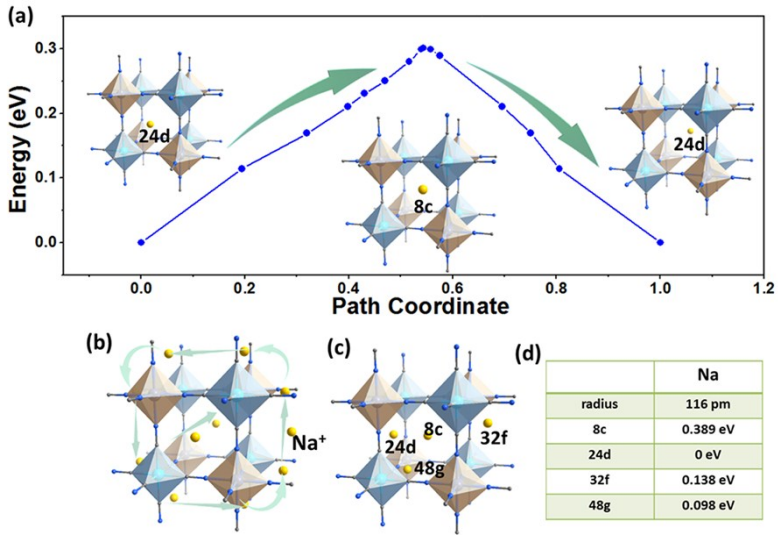

	Na
radius	116 pm
8c	0.389 eV
24d	0 eV
32f	0.138 eV
48g	0.098 eV

Fig. S1 (a) and (b) indicate the sodium diffusion direction together with the energy barrier. (c) and (d) present the possible Na-ion accommodation sites and relative binding energy.

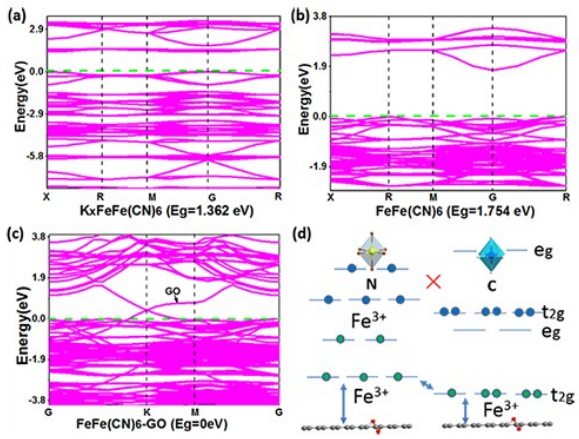

Fig. S2. (a), (b) and (c) indicate the band structure of $K_{0.33}FeFe(CN)_6$, $FeFe(CN)_6$, together with the $FeFe(CN)_6$/RGO. (d)shows the presence of RGO could facilitate the electronic diffusion, thus leading to better electrochemical performance.

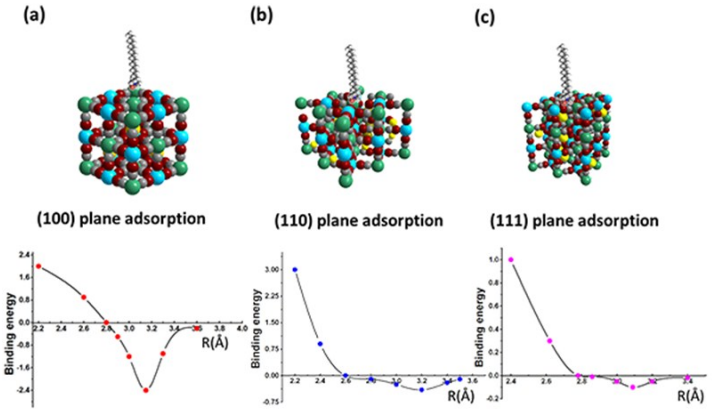

Fig. S3. CTAB adsorption on the (100), (110), (111) plane of $K_{0.33}FeFe(CN)_6$ and the corresponding energy adsorption curves.

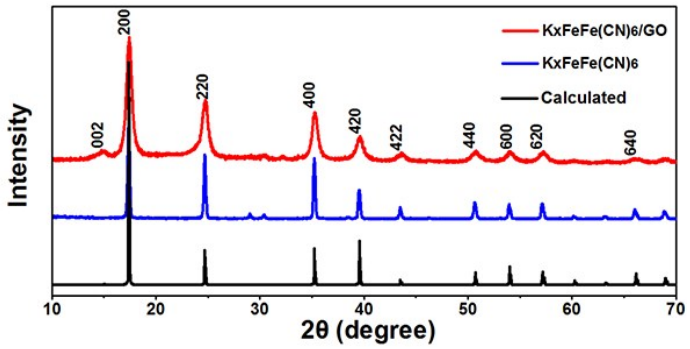

Figure S4. XRD pattern of $K_{0.33}FeFe(CN)_6$ and $K_{0.33}FeFe(CN)_6$/RGO.

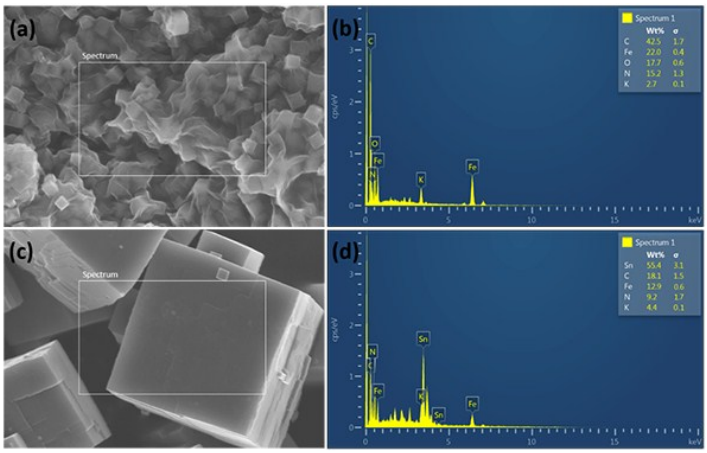

Fig. S5. EDS pattern of $K_{0.33}FeFe(CN)_6$ and $K_{0.33}FeFe(CN)_6$/RGO.

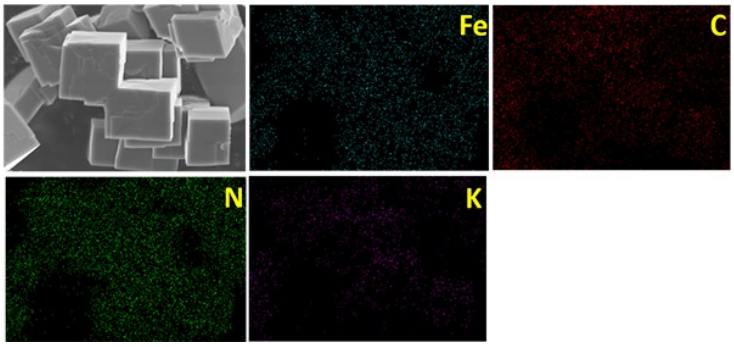

Fig. S6. Elemental mapping images of $K_{0.33}FeFe(CN)_6$.

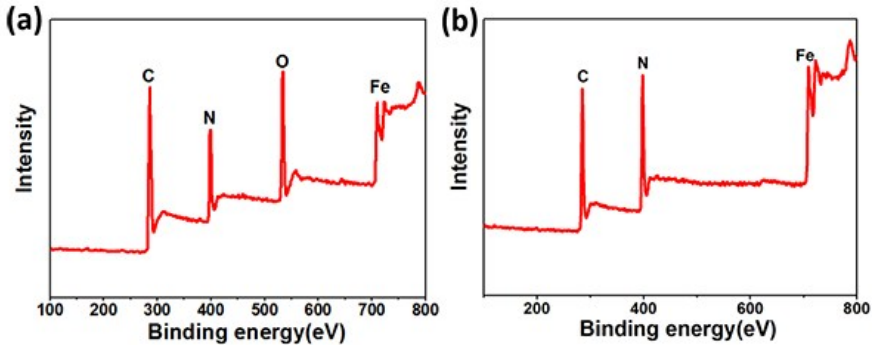

Fig. S7. XPS survey spectra of $K_{0.33}FeFe(CN)_6$ and $K_{0.33}FeFe(CN)_6$/RGO.

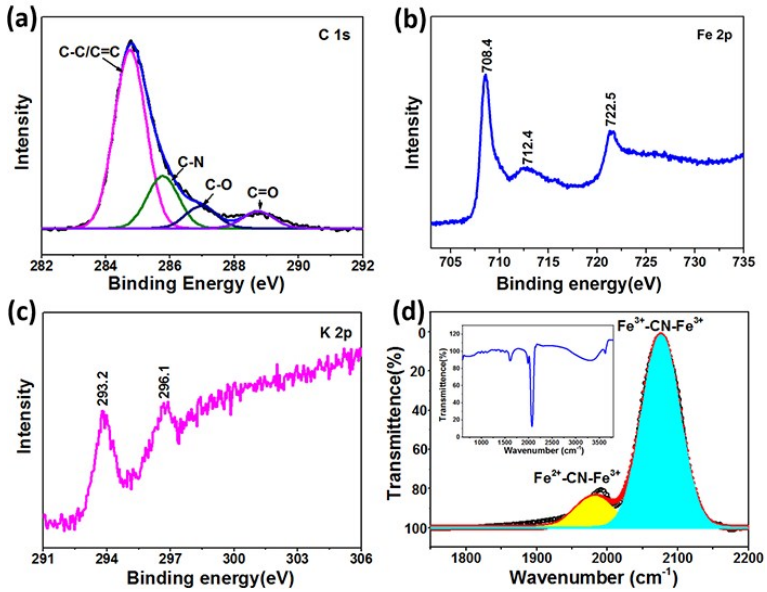

Fig. S8. (a) C 1s spectra. (b) Fe 2p spectra. (c) K 2p spectra. (d) FT-IR spectra of $K_{0.33}FeFe(CN)_6$/RGO.

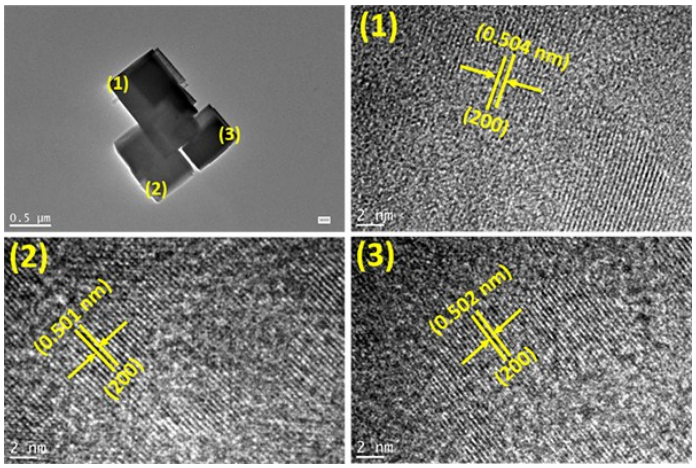

Fig.S9. HRTEM images of $K_{0.33}FeFe(CN)_6$ micro cubes under low and high resolution.

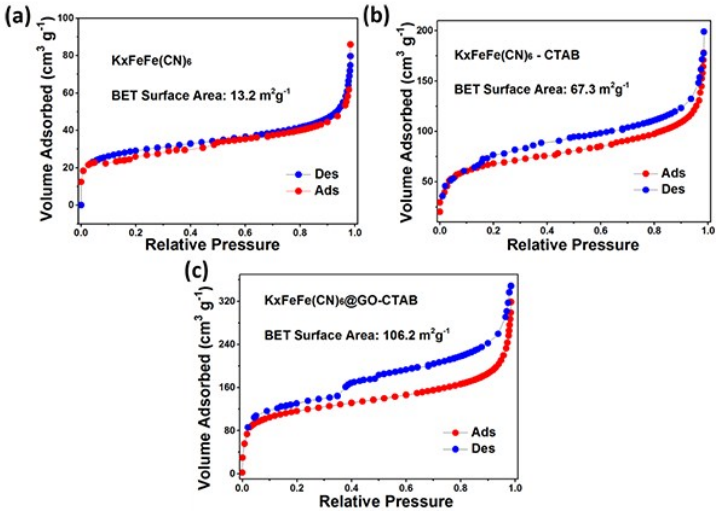

Fig. S10. BET surface of irregular-shaped $K_{0.33}FeFe(CN)_6$, $K_{0.33}FeFe(CN)_6$ micro cube, $K_{0.33}FeFe(CN)_6$/RGO.

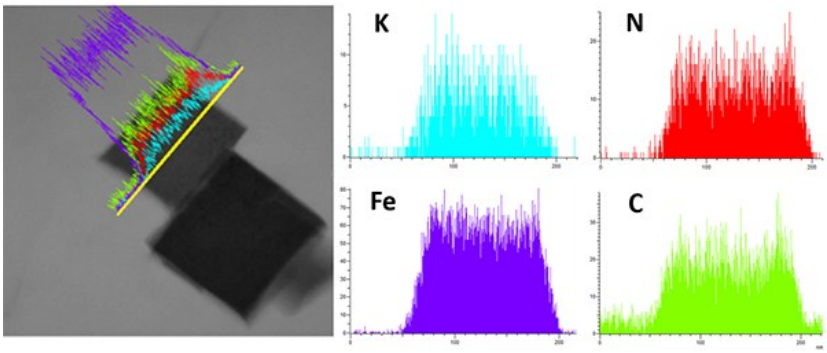

Fig. S11. Energy dispersive X-ray spectroscopy (EDX) line scans of $K_{0.33}FeFe(CN)_6$/RGO.

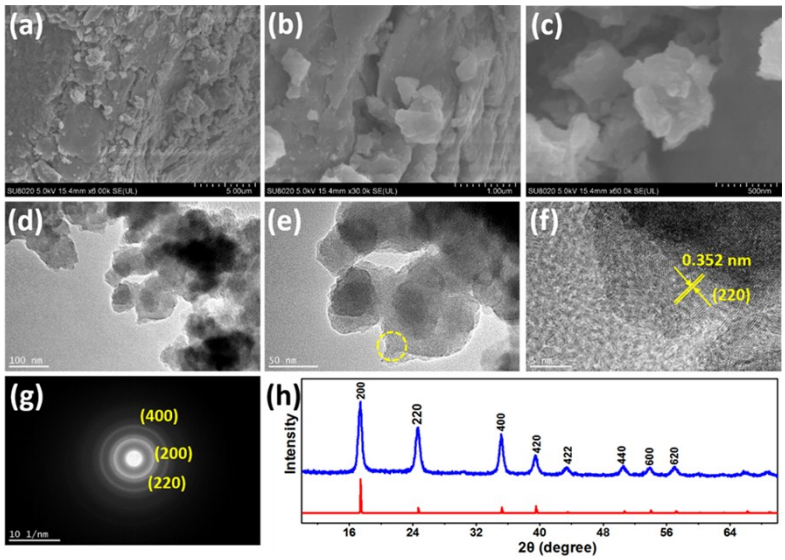

Fig. S12. (a), (b) and (c) represent the SEM images of $K_{0.33}FeFe(CN)_6$/RGO synthsised without CTAB. (d), (e), (f) are the TEM images of $K_{0.33}FeFe(CN)_6$. (g) and (h) display the corresponding SAED and XRD pattern.

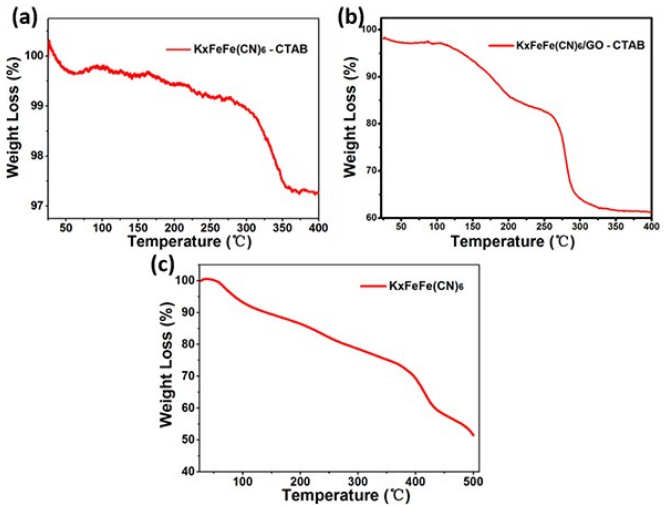

Fig. S13. TG curves of $K_{0.33}FeFe(CN)_6$ micro cube, $K_{0.33}FeFe(CN)_6$/RGO and irregular–shaped $K_{0.33}FeFe(CN)_6$ particle.

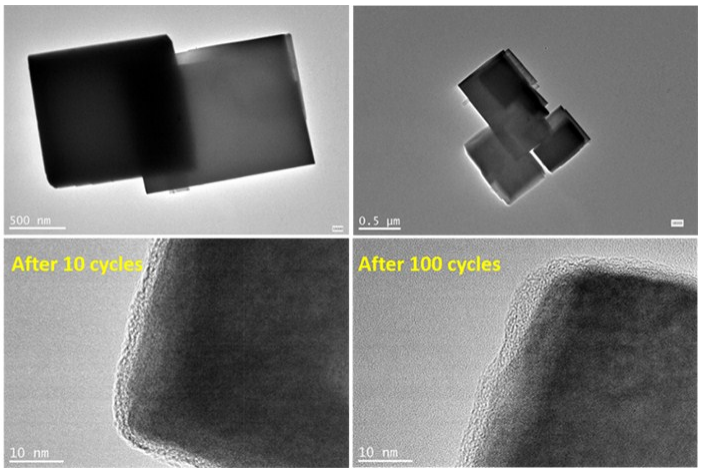

Fig. S14. TEM images of $K_{0.33}FeFe(CN)_6$ sample after 0, 10,100 cycles.

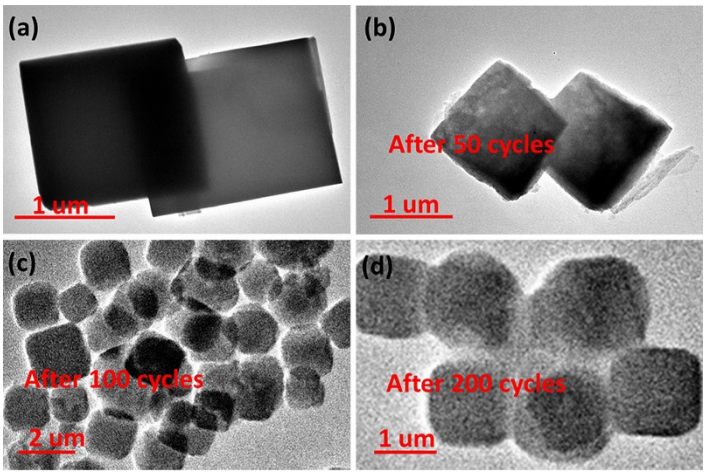

Fig. S15. (a), (b), (c) and (d) are TEM images of $K_{0.33}FeFe(CN)_6$ microcube after 50, 100, and 200 cycles respectively.

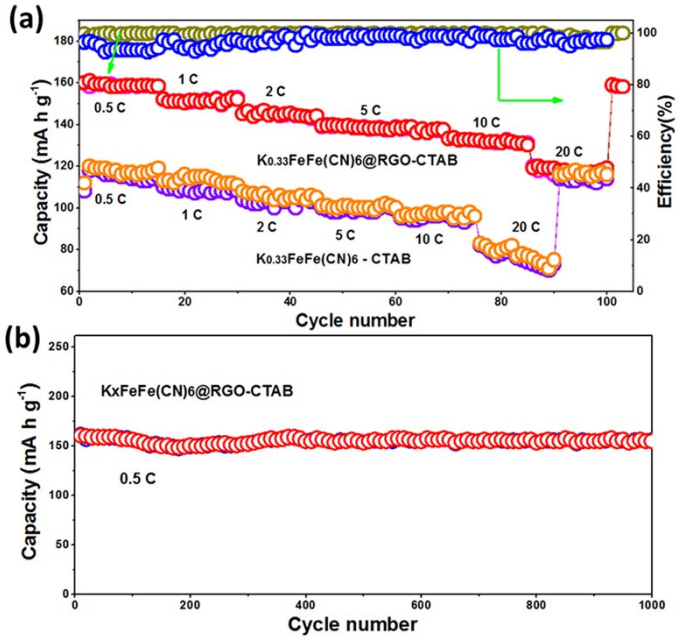

Fig. S16. (a) Rate performances of $K_{0.33}FeFe(CN)_6$/RGO nanocube and $K_{0.33}FeFe(CN)_6$ microcube . (b) Long-cycling performances of $K_{0.33}FeFe(CN)_6$/RGO nanocube at 0.5 C.

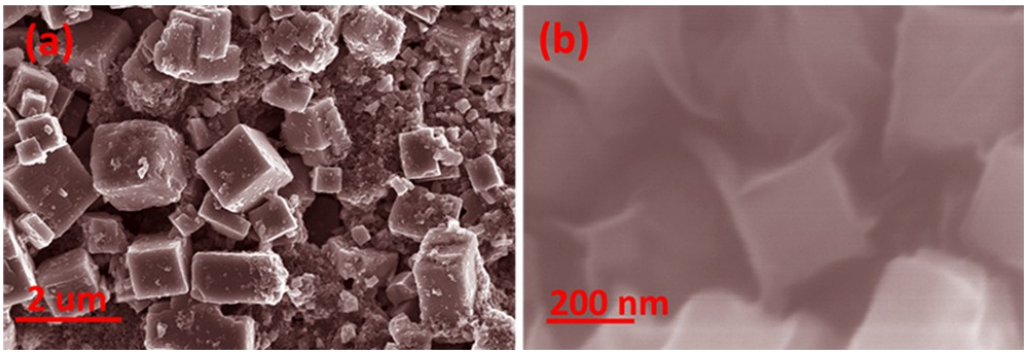

Fig.S17. (a) and (b) are SEM images of $K_{0.33}FeFe(CN)_6$ and $K_{0.33}FeFe(CN)_6$/RGO after 250 and 1000 cycles respectively.

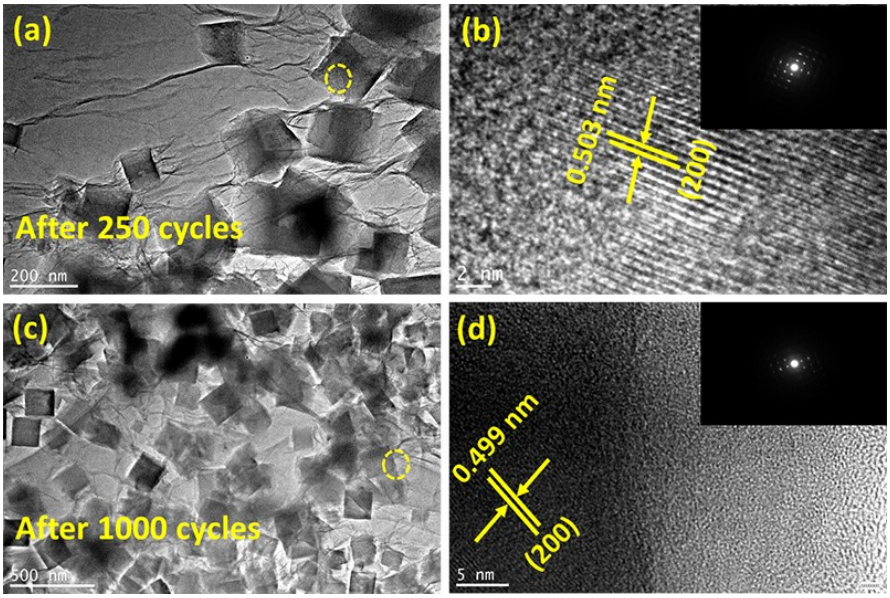

Fig.S18. (a) and (c) are TEM images of $K_{0.33}FeFe(CN)_6$/RGO after 250 and 1000 cycles respectively. (c) and (d) are HRTEM of $K_{0.33}FeFe(CN)_6$/RGO after 250 and 1000 cycles respectively, and the inset shows the corresponding SAED pattern.

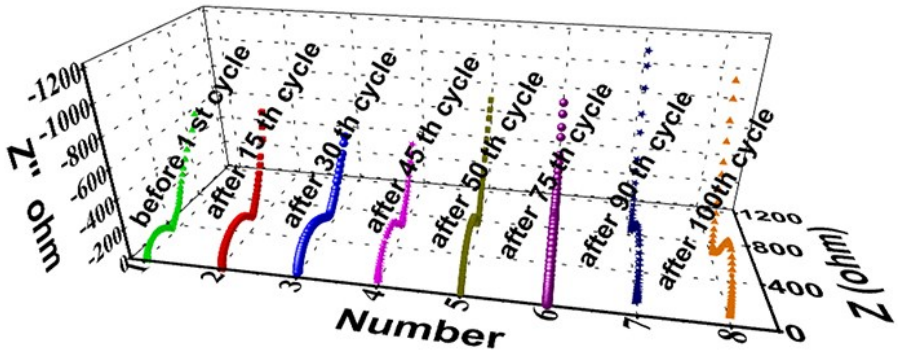

Fig. S19. Nyquist plots of the $K_{0.33}FeFe(CN)_6$/RGO nanocube electrodes.

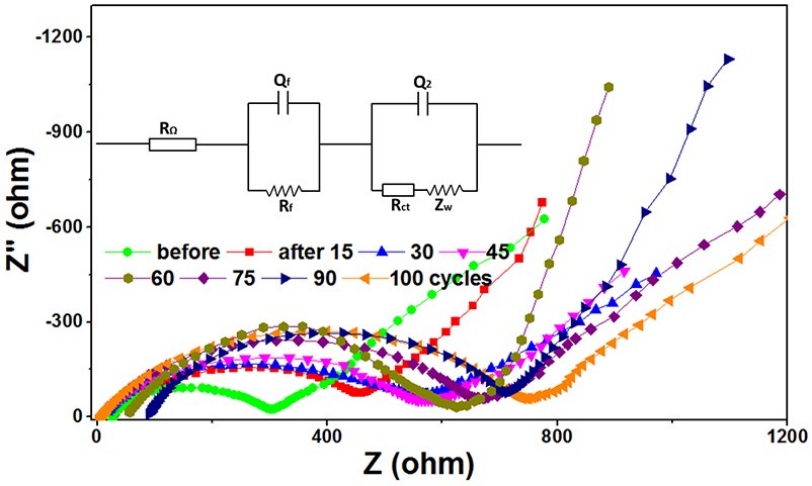

Fig. S20. Nyquist plots of the $K_{0.33}FeFe(CN)_6$/RGO nanocube electrodes and the corresponding equivalent circuit model of the studied system.

(a)

$K_{0.33}FeFe(CN)_6$	a=10.13Å	b=10.13Å	b=10.13Å	Volume=1039.51Å^3	
Atom	Wyck	x	y	z	S.O.F
Fe1	4a	0	0	0	1
Fe	4b	0.5	0	0	1
C	24e	0.19	0	0	1
N	24e	0.31	0	0	1
K	8c	0.25	0.25	0.25	0.33

(b)

$K_{0.33}Na_{1.67}FeFe(CN)_6$	a=10.2502Å	b=10.2501Å	b=10.2502Å	Volume=1076.94Å^3	
Atom	Wyck	x	y	z	S.O.F
Fe1	4a	0.001	0.001	0	1
Fe	4b	0.4995	0.0005	0	1
C	24e	0.1901	0	0	1
N	24e	0.3099	0	0	1
K	8c	0.2501	0.25	0.2498	0.33
Na	24d	0	0.2501	0.2499	0.28

Fig. S21. Structure Parameters of $K_{0.33}FeFe(CN)_6$ and $K_{0.33}Na_{1.67}FeFe(CN)_6$ simulated by DFT.

Table S1 Element contents of $K_{0.33}FeFe(CN)_6$/RGO

	K	Fe	C	N
$K_{0.33}FeFe(CN)_6$/RGO	**4.3%**	**36.8%**	**27.9%**	**27.6%**

Table S2 Summary of the representative Prussian-based cathode materials for SIBs

Typical Sample	Cycling performances	Rate performances	References
$FeFe(CN)_6$	115 mA h g^{-1} at a moderate rate of 60 mA g^{-1} after 500 cycles	78 mA h g^{-1} at 2400 mA g^{-1} (20 C)	1
PB/C	137.6 mA h g^{-1} at a moderate rate of 30 mA g^{-1} after 500 cycles	112 mA h g^{-1} at a current density of 800 mA g^{-1} (6 C)	2
PB@C	123 mA h g^{-1} at a moderate rate of 100 mA g^{-1} after 300 cycles	99 mA h g^{-1} at 2000 mA g^{-1} (20 C)	3
PB-GO	139.5 mA h g^{-1} at a moderate rate of 25 mA g^{-1} after 50 cycles	107 mA h g^{-1} at 2000 mA g^{-1} (20 C)	4
$Na_{1.40}MnFe(CN)_6$	134 mA h g^{-1} at a moderate rate of 6 mA g^{-1} after 30 cycles	73 mA h g^{-1} at 2040 mA g^{-1} (20 C)	5
$Na_{1.70}FeFe(CN)_6$	91 mA h g^{-1} at a moderate rate of 200 mA g^{-1} after 100 cycles	73.6 mA h g^{-1} at 1200 mA g^{-1} (10 C)	6
FeNiHCF	101.76 mA h g^{-1} at a moderate rate of 10 mA g^{-1} after 200 cycles	71 mA h g^{-1} at 500 mA g^{-1} (5 C)	7
$Na_{1.56}Fe[Fe(CN)_6]\cdot_{3.1}H_2O$	99.91 mA h g^{-1} at a moderate rate of 20 mA g^{-1} after 400 cycles	90 mA h g^{-1} at 100 mA g^{-1} (1 C)	8
FeHCF	100.1 mA h g^{-1} at a moderate rate of 100 mA g^{-1} after 70 cycles	108 mA h g^{-1} at 100 mA g^{-1} (1 C)	9
$Na_{0.61}Fe[Fe(CN)_6]_{0.94}$	170.1 mA h g^{-1} at a moderate rate of 25 mA g^{-1} after 150 cycles	70 mA h g^{-1} at 600 mA g^{-1} (5 C)	10
R-$Na_{1.92}Fe[Fe(CN)_6]$	117.54 mA h g^{-1} at a moderate rate of 10 mA g^{-1} after 50 cycles	77 mA h g^{-1} at 500 mA g^{-1} (5 C)	11
$K_{0.33}FeFe(CN)_6$-RGO	148.44 mA h g^{-1} at a moderate rate of 86 mA g^{-1} after 1000 cycles	126 mA h g^{-1} at 2400 mA g^{-1} (20 C)	This Work

Table S3 Impedance parameters derived from using equivalent circuit model for $K_{0.33}FeFe(CN)_6$/RGO electrode.

Electrode	R_f (Ω)	Q_f (μF)	R_{ct} (Ω)	Q_2 (μF)
before 1st cycle	**300.5**	**280.4**	**200.2**	**210.6**
after 15th cycles	**450.8**	**432.7**	**208.4**	**225.3**
after 30th cycles	**547.6**	**550.4**	**210.5**	**228.9**
after 45th cycles	**565.6**	**560.2**	**223.2**	**230.3**
after 60th cycles	**620.1**	**617.3**	**230.6**	**236.6**
after 75 cycles	**625.6**	**620.8**	**240.2**	**245.3**
after 90th cycles	**640.2**	**630.7**	**260.1**	**258.3**
after 100th cycles	**680.1**	**676.3**	**270.5**	**263.4**

1 Wu, X., W. Deng, J. Qian, Y. Cao, X. Ai, H. Yang, *J.Mater.Chem.A*, 2013, **1,** 10130-10134**.**

2 Dezhi, Y., X. Jing, L. Xiao-Zhen, W. Hong, H. Yu-Shi, M. Zi-Feng, *Chemical Communications*, 2015, **51,** 8181-8184**.**

3 Jiang, Y., S. Yu, B. Wang, Y. Li, W. Sun, Y. Lu, M. Yan, B. Song, S. Dou, *Advanced Functional Materials*, 2016*, DOI: 10.1002/adfm.201600747*

4 Prabakar, S.R., J. Jeong, M. Pyo, *RSC Advances*, 2015, **5,** 37545-37552**.**

5 Wang, L., Y. Lu, J. Liu, M. Xu, J. Cheng, D. Zhang, J.B. Goodenough, *Angewandte Chemie International Edition*, 2013, **52,** 1964-1967**.**

6 Liu, Y., Y. Qiao, W. Zhang, Z. Li, X. Ji, L. Miao, L. Yuan, X. Hu, Y. Huang, *Nano Energy*, 2015, **12,** 386–393**.**

7 Yu, S., Y. Li, Y. Lu, B. Xu, Q. Wang, M. Yan, Y. Jiang, *Journal of Power Sources*, 2015, **275,** 45-49**.**

8 Li, W.J., S.L. Chou, J.Z. Wang, Y.M. Kang, J.L. Wang, Y. Liu, Q.F. Gu, H.K. Liu, S.X. Dou, *Chemistry of Materials*, 2015, **27,** 1997-2003**.**

9 Yu, S.-H., M. Shokouhimehr, T. Hyeon, Y.-E. Sung, *ECS Electrochemistry Letters*, 2013, **2,** A39-A41**.**

10 You, Y., X.L. Wu, Y.X. Yin, Y.G. Guo, *Energy Environ Sci*, 2014, **7,** 1643-1647**.**

11 Song, J., L. Wang, Y. Lu, J. Liu, B. Guo, P. Xiao, J.-J. Lee, X.-Q. Yang, G. Henkelman, J.B. Goodenough, *Journal of the American Chemical Society*, 2015, **137,** 2658-2664**.**